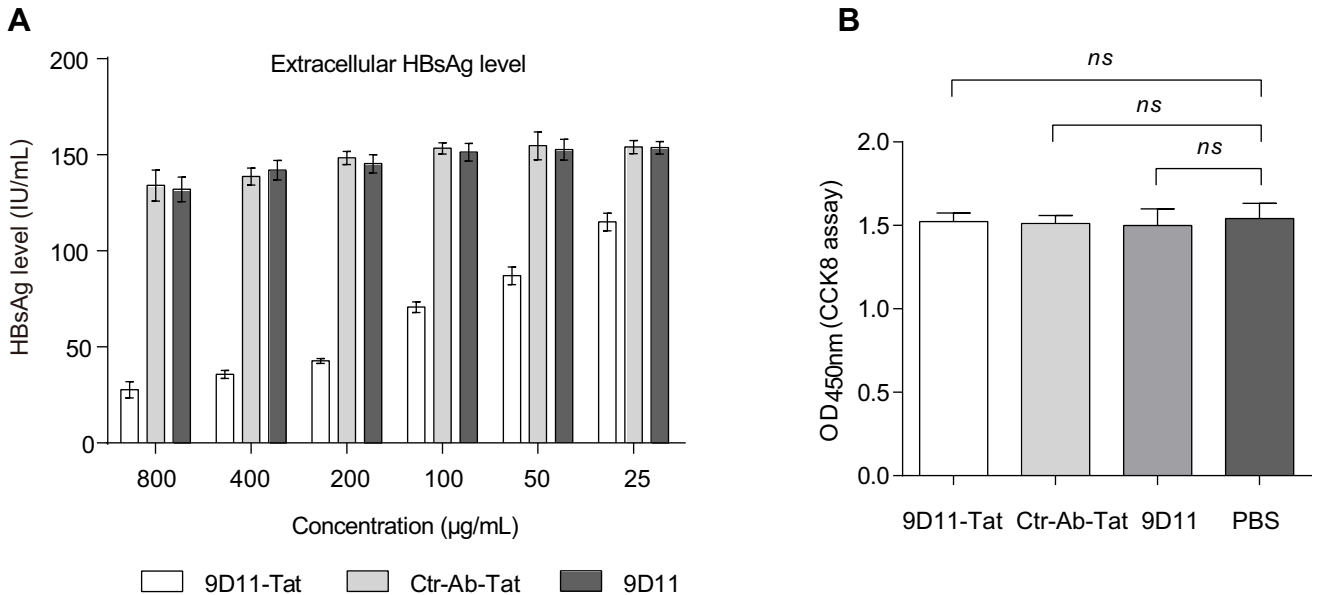

Figure S1. Evaluations of dose-dependentanti-HBV effect (A) and potential cytotoxicity (B) of 9D11-Tat

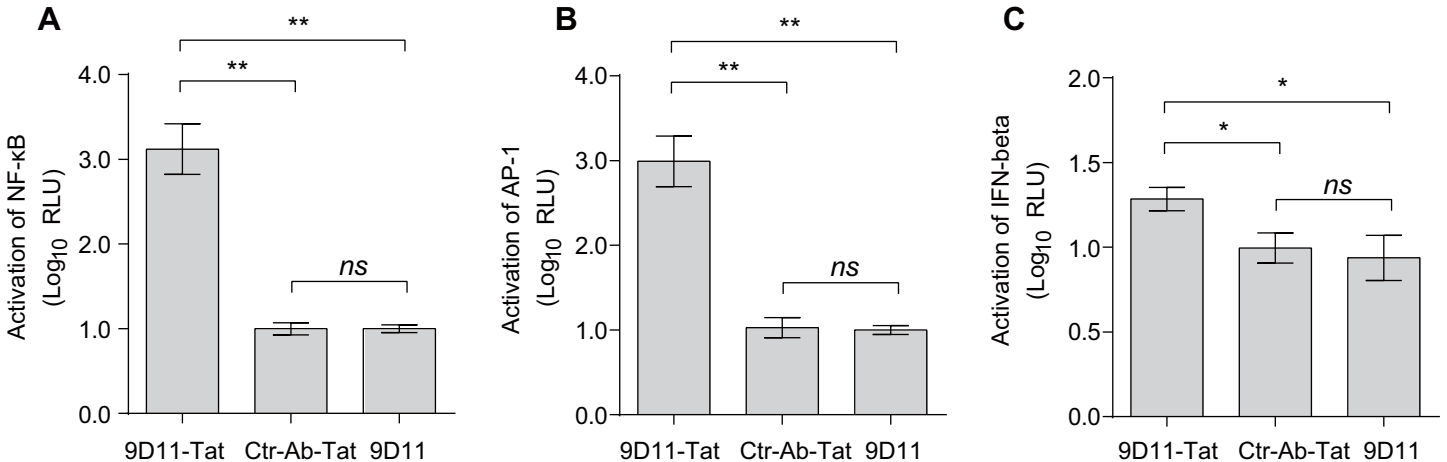

Figure S2. Influence of 9D11-Tat on the promoter activities of NF-κB (A), AP1 (B), and IFN-β (C)

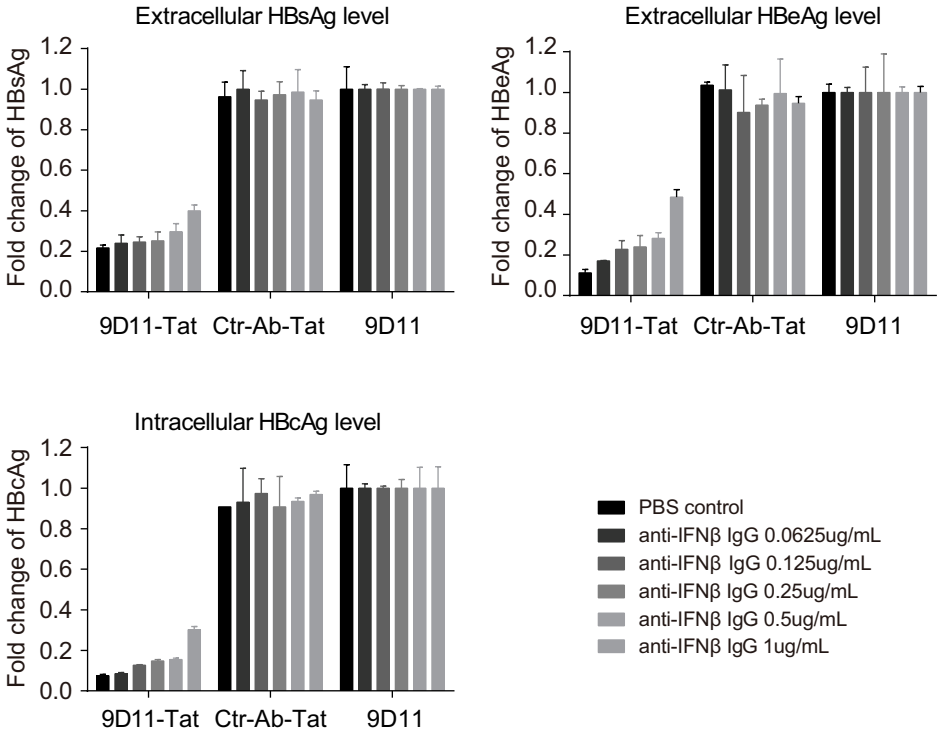

Figure S3. Anti-IFN-β neutralizing antibody could partially reverse 9D11-Tat-mediated HBV suppression

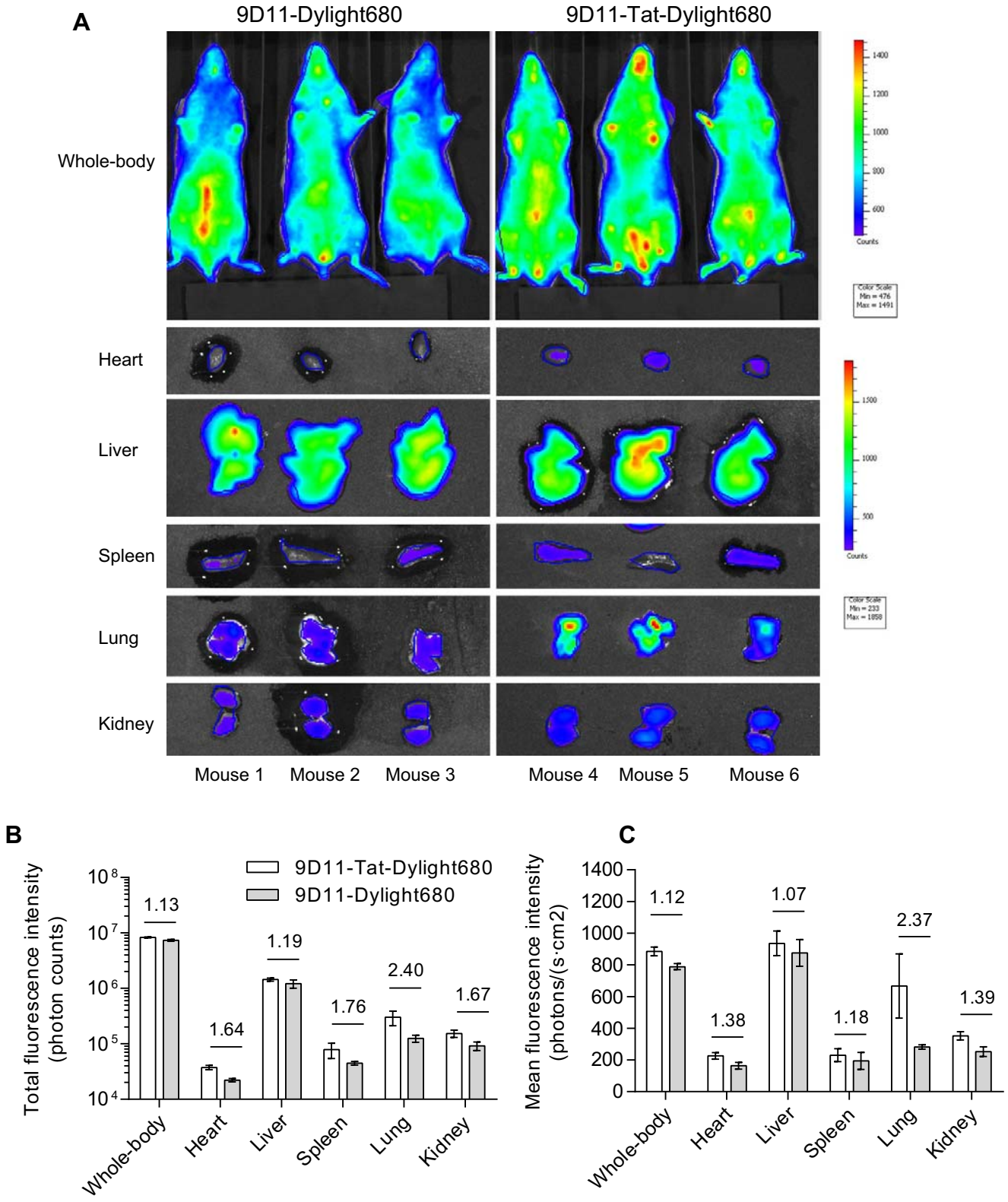

Figure S4. In vivo tracking of 9D11 and 9D11-Tat antibody distributions with near-infrared fluorescent dyes in HBV-Tg mice

Supplementary Table S1. Amino acid sequence of 9D11 antibody variants.

	amino acid sequence
9D11 antibody H Chain V region	QVQLQQPGAELVRPGASVKLSCKASGYSFTSFWISWVKQ RPGQGLEWIAMIHPSDNGIRFNQKFKDKATLTVDKSSSTA YMQLNSPTSEDSAVYFCARAGTATFTYWGQGTLVTVSA
9D11 antibody L Chain V region	DIQMTQTTSSLSVSLGDRVTISCRASQDISNYLNWYQQKP DGIVKLLIYYTSRLHSGVPSRFSGSGSGTDYSLTISNLEQE DLATYFCQQGNALPWTFGGGTKLEIKRA
H chain sequence of 9D11-Tat (Tat sequence was underline is Tat)	QVQLQQPGAELVRPGASVKLSCKASGYSFTSFWISWVKQ RPGQGLEWIAMIHPSDNGIRFNQKFKDKATLTVDKSSSTA YMQLNSPTSEDSAVYFCARAGTATFTYWGQGTLVTVSAA RPTPPSVYPLAPGSAAQTNSMVTLGCLVKGYFPEPVTVT WNSGSLSSGVHTFPAVLQSDLYTLSSSVTVPSSTWPSET VTCNVAHPASSTKVDKKIVPRDCGCKPCICTVPEVSSVFIF PPKPKDVLTITLTPKVTCVVVDISKDDPEVQFSWFVDDVEV HTAQTQPREEQFNSTFRSVSELPIMHQDWLNGKEFKCRV NSAAFPAPIEKTISKTKGRPKAPQVYTIPPPKEQMAKDKVS LTCMITDFFPEDITVEWQWNGQPAENYKNTQPIMDTDGS YFVYSKLNVQKSNWEAGNTFTCSVLHEGLHNHHTEKSLS HSPGKGRKKRRQRRRPPQ
H chain sequence of 9D11-Tat-CH3$^{-/-}$	QVQLQQPGAELVRPGASVKLSCKASGYSFTSFWISWVKQ RPGQGLEWIAMIHPSDNGIRFNQKFKDKATLTVDKSSSTA

(Tat sequence was underline is Tat)	YMQLNSPTSEDSAVYFCARAGTATFTYWGQGTLVTVSAA RPTPPSVYPLAPGSAAQTNSMVTLGCLVKGYFPEPVTVT WNSGSLSSGVHTFPAVLQSDLYTLSSSVTVPSSTWPSET VTCNVAHPASSTKVDKKIVPRDCGCKPCICTVPEVSSVFIF PPKPKDVLTITLTPKVTCVVVDISKDDPEVQFSWFVDDVEV HTAQTQPREEQFNSTFRSVSELPIMHQDWLNGKEFKCRV NSAAFPAPIEKTISKTKGRKKRRQRRRPPQ
H chain sequence of 9D11-Tat-Mut (Tat sequence was underline is Tat, H433A, N434A and H435A mutations were indicated at red)	QVQLQQPGAELVRPGASVKLSCKASGYSFTSFWISWVKQ RPGQGLEWIAMIHPSDNGIRFNQKFKDKATLTVDKSSSTA YMQLNSPTSEDSAVYFCARAGTATFTYWGQGTLVTVSAA RPTPPSVYPLAPGSAAQTNSMVTLGCLVKGYFPEPVTVT WNSGSLSSGVHTFPAVLQSDLYTLSSSVTVPSSTWPSET VTCNVAHPASSTKVDKKIVPRDCGCKPCICTVPEVSSVFIF PPKPKDVLTITLTPKVTCVVVDISKDDPEVQFSWFVDDVEV HTAQTQPREEQFNSTFRSVSELPIMHQDWLNGKEFKCRV NSAAFPAPIEKTISKTKGRPKAPQVYTIPPPKEQMAKDKVS LTCMITDFFPEDITVEWQWNGQPAENYKNTQPIMDTDGS YFVYSKLNVQKSNWEAGNTFTCSVLHEGLAAAHTEKSLS HSPGKGRKKRRQRRRPPQ

Supplementary Table S2. Sequence of siRNA

ID	Sequence of siRNA
TRIM21-1	UGGCAUGGAGGCACCUGAAGGUGG
TRIM21-2	UCAUUGUCAAGCGUGCUGC
Control siRNA	UUCUCCGAACGUGUCACGUTT

Supplemental Figure 1. Evaluations of dose-dependent anti-HBV effect (A) and potential cytotoxicity (B) of 9D11-Tat. The HBV48-WT-transfected Huh7 cells were treated with a series of two-fold dilutions of 9D11-Tat, Ctr-Ab-Tat, and 9D11. Two days after treatments, the extracellular HBsAg levels were measured and were expressed as the mean ± SD. For evaluation of potential cytotoxicity, Huh7 cells that treated with different mAbs at a concentration of 400 μg/mL. Two days after treatments, the culture medium was collected for CCK assays. The data represent mean ± SD from three independent experiments.

Supplemental Figure 2. Influence of 9D11-Tat on the promoter activities of NF-κB (A), AP1 (B) and IFN-β (C). Huh7 cells that transfected with HBV48-WT and luciferase reporter vectors of NF-κB, AP1 or IFN-β were treated with 9D11-Tat, Ctr Ab-Tat and 9D11 mAbs, respectively. Two days after treatments the cells were collected for intracellular luciferase measurements. The data represent mean ± SD from three independent experiments.

Supplemental Figure 3. Anti-IFN-β neutralizing antibody could partially reverse 9D11-Tat-mediated HBV suppression. Dose-dependent (0.0625 μg/mL to 1.0 μg/mL) blocking effects of anti-IFN-β neutralizing antibody to 9D11-Tat mediated inhibitions on HBsAg (A), HBeAg (B), and HBcAg (C). The data represent mean ± SD from three independent tests for each concentration.

Supplemental Figure 4. In vivo tracking of 9D11 and 9D11-Tat antibody

distributions with near-infrared fluorescent dyes in HBV-Tg mice. Dylight680 labeled 9D11-Tat and 9D11 (5 mg/kg) were injected into HBV-Tg mice. (A) Fluorescence images of whole animals and isolated tissues harvested at 24 h after mAb infusions. Semi-quantitative analyses of (A) using the software package included with the *in vivo* imaging system on total (B) and mean (C) fluorescence intensity. The average fold-change number between 9D11-Tat and 9D11 group is indicated on the bar.